Use of hourly Geostationary Operational Environmental Satellite (GOES) fire emissions in a Community Multiscale Air Quality (CMAQ) model for improving surface particulate matter predictions

Eun-Su Yang,[1] Sundar A. Christopher,[1,2] Shobha Kondragunta,[3] and Xiaoyang Zhang[3,4]

Received 11 May 2010; revised 1 December 2010; accepted 17 December 2010; published 17 February 2011.

[1] Large changes in surface-level $PM_{2.5}$ concentrations and columnar aerosol optical thickness (AOT) were observed downwind of fires that originated in Georgia and Florida during the April–May 2007 period. In order to quantify the impacts of these wildfires on particulate matter air quality, Community Multiscale Air Quality (CMAQ) simulations were conducted by adding hourly fire emissions derived from the Geostationary Operational Environmental Satellite (GOES) imagers. The simulations include ambient aerosols by accounting for background emissions using the Sparse Matrix Operator Kernel Emissions (SMOKE) model. The impacts of fire emissions are obtained by comparing the CMAQ simulations with and without fire emissions. Overall, the CMAQ-derived $PM_{2.5}$ reproduces the major smoke transport features of the Moderate Resolution Imaging Spectrometer (MODIS) AOT, but is systematically lower than the ground-based observations of $PM_{2.5}$ mass concentrations during the fires. An increase of the satellite-derived fire emissions improves the simulated magnitude of $PM_{2.5}$ concentrations. We also show that the disagreement between the CMAQ predictions and ground-based observations during the high $PM_{2.5}$ episodes occurs when the predicted position of fire plume is not accurately located. The smoke position error grows more rapidly due to drift behavior of model wind error, so the position error dominates the accuracy of site-specific CMAQ $PM_{2.5}$ predictions.

Citation: Yang, E.-S., S. A. Christopher, S. Kondragunta, and X. Zhang (2011), Use of hourly Geostationary Operational Environmental Satellite (GOES) fire emissions in a Community Multiscale Air Quality (CMAQ) model for improving surface particulate matter predictions, *J. Geophys. Res.*, *116*, D04303, doi:10.1029/2010JD014482.

1. Introduction

[2] The Community Multiscale Air Quality (CMAQ) model has been extensively used to assess air quality on a large range of time scales from minutes to days to weeks and months as well as on numerous spatial scales ranging from local to regional to continental [e.g., *Byun and Schere*, 2006; *Marmur et al.*, 2006; *Zhang et al.*, 2009]. To ensure its successful application to particulate matter (PM) air quality forecasts, the CMAQ modeling system requires accurate information about emission source functions [e.g., *Roy et al.*, 2007]. Among the emission sources, it should be noted that wildfires are episodic events. Since fire times, locations, and emission rates are available on a near-real time basis from spaceborne sensors, the CMAQ could be used to assess and forecast PM air quality during fire events. To examine the use of satellite-derived fire emissions in CMAQ we study the Georgia and Florida fires of April and May 2007 that were among the largest wildfires in the history of Georgia and Florida. In May 2007, the abnormally dry conditions continued over Georgia and Florida during the month except light rainfall reported at some coastal locations in North Carolina and Florida from the subtropical storm Andrea on 9–11 May 2007. This drought exacerbated wildfire conditions, with 192,000 ha in Georgia and 93,000 ha in Florida burned. A remote sensing perspective of these fires is fully discussed by *Christopher et al.* [2009].

[3] We explore the use of satellite-based fire locations and emissions in the CMAQ model to assess whether CMAQ simulations improve predicted $PM_{2.5}$ mass (PM with an aerodynamic diameter less than 2.5 μm) concentrations near and downwind of fires. Previous studies [*Rolph et al.*, 2009; *Stein et al.*, 2009] accounted for fire emissions estimated with the U. S. Forest Service's BlueSky [*Larkin et al.*, 2009] and generated advection and dispersion of smoke plume

[1]Earth System Science Center, University of Alabama in Huntsville, Huntsville, Alabama, USA.
[2]Department of Atmospheric Science, University of Alabama in Huntsville, Huntsville, Alabama, USA.
[3]Center for Satellite Applications and Research, NESDIS, NOAA, Camp Springs, Maryland, USA.
[4]Earth Resources Technology Inc., Laurel, Maryland, USA.

Copyright 2011 by the American Geophysical Union.
0148-0227/11/2010JD014482

from the Hybrid Single Particle Lagrangian Integrated Trajectory (HYSPLIT) model [*Draxler and Hess*, 1997]. *Rolph et al.* [2009] estimated gross particle emissions based on an average rate of 68 kg h^{-1} ha^{-1} with daily information on burned areas. Alternatively, the fire emissions were estimated using aerosol optical thickness (AOT) from the Moderate Resolution Imaging Spectrometer (MODIS) [*Mathur*, 2008]. By assimilating aerosol optical depths (AOD) from the MODIS into the CMAQ to assess $PM_{2.5}$ mass concentrations due to fires, *Mathur* [2008] demonstrated the significant improvement of surface-level $PM_{2.5}$ compared to the simulations without MODIS AOD assimilations. The observed spatial variability in surface-level $PM_{2.5}$ was also well predicted because the spatial distribution of the retrieved MODIS AOD already reflected the long-range transport of PM at the MODIS overpass time.

[4] However, the MODIS AOD is available only for clear sky conditions and only twice a day for both Terra and Aqua. The initialization of $PM_{2.5}$ burden from MODIS AOD could not account for fire emissions for the cases with missing MODIS AOD, under cloudy conditions, and before and after the MODIS overpass time. The fire detection using the GOES imagery, on the contrary, is more frequent (half hour) and can improve temporal and spatial allocation of emissions from fires. Since the GOES fire detection algorithm is limited to providing emission strengths, locations and timing of hot spots, spatial distribution of $PM_{2.5}$ is subject to uncertainties in transport and mixing processes of fire plume.

[5] In this study, we use the CMAQ modeling system that consists of three primary modeling components including the PSU/NCAR mesoscale model (MM5, version 3.7 [*Grell et al.*, 1995]) to reproduce meteorological conditions, Sparse Matrix Operator Kernel Emissions model (SMOKE, version 2.34 [*Houyoux et al.*, 2000]) to generate background emissions from natural and anthropogenic sources, and CMAQ (version 4.6) to simulate atmospheric gases and particulate matter. CMAQ model simulations include background emissions as well as fire emissions to attribute the amount of $PM_{2.5}$ from wildfires, where the contribution of background emissions to the measured $PM_{2.5}$ could be important in an urban area [e.g., *Edgerton et al.*, 2005; *Stein et al.*, 2009]. The background emission estimates are based on the 2002 National Emission Inventory (NEI). The MM5, SMOKE, and CMAQ models are described in detail in section 3, and the method to estimate fire emissions from satellite measurements is presented in section 2.1.

[6] The transport of fire plumes is also an important factor to accurately forecast $PM_{2.5}$ mass concentrations because fire plumes rise, change direction, and move downwind for a few hours to days depending on atmospheric conditions. The uncertainty in simulated locations of fire plumes gradually increases over time in the boundary layer where winds are quite variable and most uncertain. Errors in wind speed and wind direction propagate into travel distance and direction of fire plumes by increasing uncertainty in predicted paths of fire plumes. This study evaluates transport error driven by the MM5 winds during the CMAQ transport process. In order to grasp the characteristics of uncertainty in transport, we investigate how uncertainty in winds propagates into deviations of predicted fire plumes from the actual location and how the CMAQ simulations capture the elevated values of $PM_{2.5}$ mass concentrations during fires by comparing them with the ground-based $PM_{2.5}$ observations.

[7] This study focuses on $PM_{2.5}$, one of the seven EPA criteria pollutants. Due to the public health issue related to short-term and long-term exposure of these particles, the U.S. EPA in 2006 lowered the permissible 24 h level of $PM_{2.5}$ from 65 to 35 $\mu g\ m^{-3}$. CMAQ simulations are performed with a base case emissions and with added fire emissions to assess the impact on predicted $PM_{2.5}$ due to wildfires. The results are compared with satellite and ground-based data to evaluate responses of CMAQ simulations for various input parameters such as fire emission rates and wind fields.

2. Data

[8] The GOES biomass burning emission estimates are used as emission inputs to the CMAQ model. By combining them with the background emissions, the CMAQ simulates $PM_{2.5}$ mass concentrations. The major smoke features simulated by CMAQ are compared with the MODIS AOT and the Atmospheric Infrared Sounder (AIRS) total column CO (TCO). The AirNow and Interagency Monitoring of Protected Visual Environments (IMPROVE) $PM_{2.5}$ measurements are used for site-specific comparisons with the CMAQ surface-level $PM_{2.5}$. This section describes the GOES fire emission estimates, satellite-retrieved AOT and TCO, and ground-based $PM_{2.5}$ data sets.

2.1. Fire Emissions

[9] Operational forecasting from CMAQ or other air quality models requires near real time availability of biomass burning emissions. Ground reporting of fires and emission estimates is typically used for retrospective analysis rather than for forecasting purpose. Satellite data are able to meet the requirement of operational forecasting. Remotely sensed fires from NOAA operational Geostationary Operational Environmental Satellite (GOES) are widely used for hazard monitoring [*Ruminski and Kondragunta*, 2006]. Further NOAA expanded this capability by developing GOES biomass burning emissions product (GBBEP) that became operational in July 2008. Although the product has been evaluated for accuracy and tested for internal consistency before becoming operational [*Zhang et al.*, 2008], it has not been tested for applications in air quality models.

[10] The algorithm of GOES biomass burning emission estimates follows the conventional approach. This approach computes emissions using area burned (ha), fuel load (kgC/ha), emissions factors (g/kgC), and fraction of fuel consumed [*Seiler and Crutzen*, 1980]. All the parameters except emission factors are obtained from satellites. GOES satellite provides fire hot spots and instantaneous fire size information from which burned area is derived [*Zhang and Kondragunta*, 2008]. Fuel load is derived from the MODIS land products of vegetation properties [*Zhang and Kondragunta*, 2008]. Emission factors for trace gases (CO, NO_X, TNMHC, SO_2, etc.) and aerosols ($PM_{2.5}$) are obtained from the literature [*Zhang et al.*, 2008, and references therein]. The fraction of fuel consumed is a function of fuel moisture condition

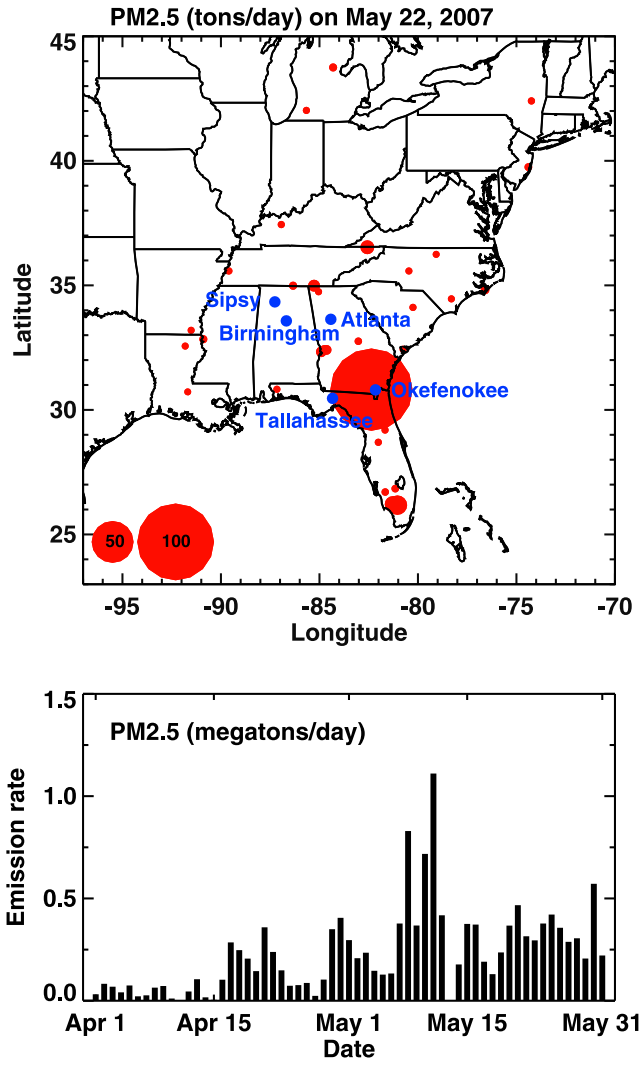

Figure 1. (top) Daily $PM_{2.5}$ emission rates in tons obtained from GBBEP on 22 May 2007. The size of circle indicates the magnitude of emission rates. Locations of three AirNow (Birmingham, Atlanta, and Tallahassee) and two IMPROVE (Okefenokee and Sipsy) stations are shown in blue dots. (bottom) Daily $PM_{2.5}$ emission rates in megatons for April–May 2007 over the model domain.

which is derived from NOAA Advanced Very High Resolution Radiometer (AVHRR) vegetation index information [*Zhang et al.*, 2008]. The burned areas at a 30 min interval are retrieved from diurnal variations of fire observations from GOES-East. By integrating all these parameters, GBBEP algorithm runs every day on all observed fire hot spots over the CONtiguous United States (CONUS) to compute emissions every half hour. The output emissions data are integrated to hourly time scale and are publicly available (ftp://satepsanone.nesdis.noaa.gov/EPA/GBBEP/).

[11] The species of trace gases and aerosols in GBBEP are $PM_{2.5}$, CO, NO_2, NH_3, SO_2, CH_4, NO_X, and nonmethane hydrocarbons (NMHC). Among them, $PM_{2.5}$, NO_X, and NMHC are disaggregated into the appropriate CMAQ species. Figure 1 shows our model domain and the GBBEP-derived daily $PM_{2.5}$ emission rates in tons d^{-1} on 22 May 2007. The derived daily $PM_{2.5}$ emission rates over the model domain for April–May 2007 are shown as a histogram in Figure 1 (bottom).

2.2. MODIS AOT and AIRS TCO

[12] The columnar sum of aerosol extinction is retrieved as AOT from MODIS on the Terra and Aqua satellites. The MODIS instrument has near daily global coverage with a swath width of 2330 km. Because surface-level $PM_{2.5}$ is strongly related to AOT [e.g., *Al-Saadi et al.*, 2005; *Gupta and Christopher*, 2008], we collect MODIS level 2 (L2) aerosol optical thickness product (collection 5). The MODIS AOT has a spatial resolution of 10 × 10 km at nadir with the uncertainty of $\pm(0.05 + 0.15 \times \text{AOT})$ in the 0.55 μm channel [*Remer et al.*, 2005]. The MODIS data often contain large areas of missing values, especially during the fires, due to the presence of clouds, copresence of fire plumes and clouds, and misclassification of fire plumes as clouds.

[13] The smoke can also be observed in the AIRS total column CO (TCO) observations due to the AIRS cloud-clearing methodology and infrared spectral coverage [*Susskind et al.*, 2003]. The Atmospheric Infrared Sounder (AIRS) aboard the Earth Observing System (EOS) Aqua satellite provides near real time CO retrievals twice daily at a nadir resolution of 13.5 km. AIRS CO retrievals utilize outgoing radiances in the IR spectral bands, 4.50–4.58 μm. The AIRS CO retrievals are sensitive to CO changes in the lower midtroposphere (800 to 500 hPa) and are used for investigating long-range transport of CO from wildfires [e.g., *McMillan et al.*, 2008]. In this study, we use the integrated column amount of CO from the top of the atmosphere to the surface (AIRS version 5).

2.3. AirNow and Interagency Monitoring of Protected Visual Environments $PM_{2.5}$

[14] The $PM_{2.5}$ mass measurements from the U.S. Environmental Protection Agency (USEPA) AirNow network are used for site-specific comparison with the CMAQ $PM_{2.5}$ simulations. The $PM_{2.5}$ concentrations are measured using a Tapered-Element Oscillating Microbalance (TEOM) instrument with a stated accuracy of ± 1.5 $\mu g\ m^{-3}$ for hourly averages. The TEOM $PM_{2.5}$ mass concentrations could be underestimated due to the volatilization of ammonium nitrate and organic carbon [*Grover et al.*, 2005]. We collected the $PM_{2.5}$ measurements at 17 AirNow sites for April–May, 2007: 8 in Alabama, 3 in northern Florida, and 6 in Georgia. Birmingham (Alabama), Atlanta (Georgia), and Tallahassee (Florida) are shown in this study because most stations are located around these three stations. Tallahassee is located about 200 km from the major fire spots. Atlanta and Birmingham are about two and three times the distance from the major fire spots to Tallahassee.

[15] The Interagency Monitoring of Protected Visual Environments (IMPROVE) network was initiated in spring of 1988, and expanded to 165 monitoring sites across the United States [*Malm et al.*, 2004]. These sites are primarily located in national parks and wilderness areas. We obtain IMPROVE $PM_{2.5}$ measurements at two sites: one near the fire source (Okefenokee National Wildlife Refuge, 82.13°W,

30.74°N) and other far from the fire source (Sipsy Wilderness, 87.33°W, 34.34°N). At each site, sampling modules are used to collect the speciated $PM_{2.5}$ mass on every third day, with a sampling duration time of 24 h.

3. Modeling Approach

[16] The modeling system in this study consists of three primary models: MM5, SMOKE, and CMAQ. The CMAQ model simulates the three-dimensional atmospheric physical and chemical processes on transport, chemical transformation, and deposition of atmospheric pollutants during the Georgia and Florida fires in 2007. The CMAQ domain utilizes a grid of 168 by 177 grid cells with a horizontal resolution of 12 km. The MM5, SMOKE, and CMAQ models use the same vertical layer configuration. The vertical layer thickness gradually increases with height to better represent $PM_{2.5}$ formation and transport within the planetary boundary layer (PBL). We selected 21 terrain-following sigma levels for the 20 vertical layers with the model top at 50 hPa. We use the Carbon Bond IV (CB-IV) module [*Gery et al.*, 1989] with the Euler Backward Iterative (EBI) solver for gas phase chemistry [*Hertel et al.*, 1993]. In order to consider the growth and formation of $PM_{2.5}$, this gas phase chemistry is coupled with the fourth-generation CMAQ aerosol code (AE4). Chemical processes of secondary organic aerosol (SOA) formation are simulated by the chemical and aerosol modules, Carbon Bond (CB-IV) mechanism with AE4. In order to avoid large fire emissions solely into the surface layer, we assume that fire emissions are uniformly distributed from surface to PBL height. The plume injection height may cause changes in transport of fire plumes and surface-level $PM_{2.5}$ concentrations [*Stein et al.*, 2009; *Wang et al.*, 2006; *Colarco et al.*, 2004]. This topic is discussed in section 4.1.

[17] The MM5, a PSU/NCAR mesoscale model, is a limited-area, nonhydrostatic, terrain-following sigma-coordinate model designed to simulate or predict mesoscale atmospheric circulation [*Grell et al.*, 1995] (program details and download from http://www.mmm.ucar.edu/mm5). MM5 has a rich pool of physics modules for the PBL parameterization, radiation schemes, subgrid cloud parameterizations, explicit moisture physics, and land surface modeling. In this study, we use the Grell cumulus and the Blackadar PBL schemes.

[18] The SMOKE model generates model-ready emissions rates for point, area, biogenic (BEIS3.12 [*Pierce et al.*, 2002]), and mobile (MOBILE 6) sources [*Houyoux et al.*, 2000]. These baseline emissions do not include the emissions from the Georgia and Florida fires. The emissions only from the GBBEP product during the Georgia and Florida fires are hereinafter defined as the fire emissions. Area, point, and mobile source emissions were based on the 2002 NEI (www.epa.gov/ttn/chief). Since the annual baseline emissions of $PM_{2.5}$ are not significantly changed [*Barnard and Sabo*, 2008], the baseline emission data were not projected to 2007 (relative to a 2002 base inventory). The initial and boundary conditions for gas phase species are taken from the GEOS-CHEM simulations [*Bey et al.*, 2001] with 2×2.5 degree horizontal resolution, where the boundary condition varies every 3 h.

4. Results

[19] The CMAQ simulations are first performed with baseline emissions, which provide the base model run for $PM_{2.5}$ (hereinafter referred to as BASE). The simulations with baseline and fire emissions of $PM_{2.5}$ are also produced (hereinafter referred to as FIRE). The elevated $PM_{2.5}$ mass concentrations solely due to fires are calculated by subtracting the BASE $PM_{2.5}$ from the FIRE $PM_{2.5}$ mass concentrations. The CMAQ $PM_{2.5}$ is shown with the MODIS AOT from 21 to 24 May because surface-level $PM_{2.5}$ concentrations well correlate with AOT in the southeastern United States [e.g., *Engel-Cox et al.*, 2004]. Then it is directly compared with the ground-based $PM_{2.5}$ at the AirNow (Birmingham, Atlanta, and Tallahassee) and IMPROVE (Okefenokee and Sipsy) stations from 1 April to 31 May. The $PM_{2.5}$ fire emissions are adjusted using the MODIS AOT in a way to ensure one-to-one correspondence between CMAQ AOT and MODIS AOT.

4.1. CMAQ $PM_{2.5}$

[20] In late May of 2007, high-pressure systems persistently stayed over southeastern United States and off the southeast U.S. coast. Winds were mostly easterly in Georgia and Florida, turning to southerly in Alabama, Mississippi, and Tennessee, which transported smoke from fire source regions to the eastern United States. Figure 2 shows the spatial distribution of MODIS AOT (Figure 2a) and elevated surface-level $PM_{2.5}$ mass concentrations solely due to fires (FIRE – BASE, Figure 2b) at 1900 UT, 21–24 May 2007. Note that large areas of smoke are not seen in the MODIS due to the presence of clouds. The fire plumes are better seen in the AIRS total column CO (TCO) observations in Figure 2c. The fire impacts on $PM_{2.5}$ are evident far downwind of fire sources, for example, in southern Georgia in 21 May. The fire plumes continued to move to Alabama on 23 May, to Mississippi on 24 May, and to the northern U.S. states (see Figures 2b and 2c). The FIRE – BASE $PM_{2.5}$ (Figure 2b) reproduces major transport features of the fire plumes found in the MODIS AOT and AIRS TCO observations.

[21] The CMAQ simulations are compared with the surface $PM_{2.5}$ mass concentrations at three AirNow stations (Birmingham, Atlanta, and Tallahassee) and two IMPROVE stations (Sipsy and Okefenokee). Figure 3 shows the $PM_{2.5}$ mass concentrations from April to May 2007 at the AirNow and IMPROVE stations (black). The $PM_{2.5}$ concentrations for CMAQ FIRE are shown in red only if the FIRE $PM_{2.5}$ is larger than CMAQ BASE $PM_{2.5}$. Note that local background $PM_{2.5}$ emissions are also important sources of $PM_{2.5}$ in urban areas [*Christopher et al.*, 2009]. In Birmingham, for example, there were several episodes showing high $PM_{2.5}$ mass concentrations. The sporadic high concentrations of $PM_{2.5}$ are caused mostly by fire plumes transported from fire source regions, but still the $PM_{2.5}$ concentration spikes could be partially attributable to local emissions (see also the organic carbon concentrations at Birmingham in

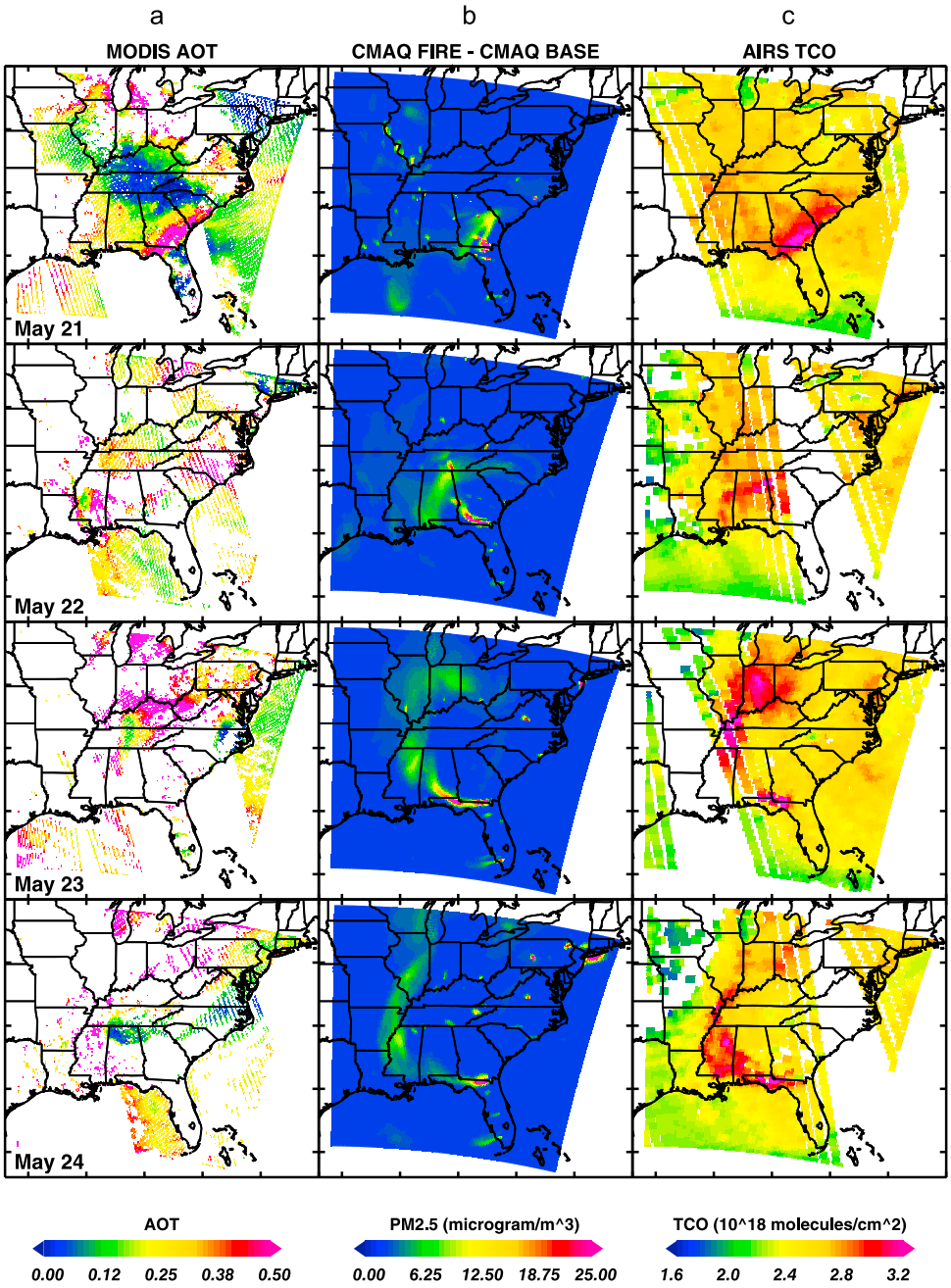

Figure 2. (b) Change in surface-level $PM_{2.5}$ concentrations due to fires in units of $\mu g\ m^{-3}$ at 1900 UT, 21–24 May 2007. The change in $PM_{2.5}$ mass concentrations are calculated by subtracting the BASE $PM_{2.5}$ from the FIRE $PM_{2.5}$ mass concentrations. For comparison, the (a) MODIS AOT and (c) AIRS TCO column density in 10^{18} molecules cm^{-2} are presented.

Figure 6). The measurements (daily averages every 3 days) at the IMPROVE stations do not provide much detail on temporal variations of $PM_{2.5}$, but the overall $PM_{2.5}$ levels are well captured by the CMAQ FIRE.

[22] Figure 3 also indicates that the CMAQ $PM_{2.5}$ simulations reproduce well the overall ambient level of $PM_{2.5}$ concentrations (blue lines). However, CMAQ $PM_{2.5}$ concentrations are far less than the ground-based observations during the fire episodes (red lines), except at the Okefenokee IMPROVE station which shows huge spikes. Besides, it seems that CMAQ FIRE does not accurately locate the fire plumes so that it often fails to capture the high $PM_{2.5}$ episodes as observed at the ground stations. Although the CMAQ simulations are not expected to predict the exact locations of fire plumes far downwind of fires (e.g., Birmingham and Atlanta), it is surprising that the CMAQ FIRE does not reproduce as much elevated $PM_{2.5}$ concentrations as the ground-based observations at Tallahassee (AirNow) and Okefenokee (IMPROVE; see 1 and 4 May in Figure 3). Note that Tallahassee and Okefenokee are near the major fire source regions.

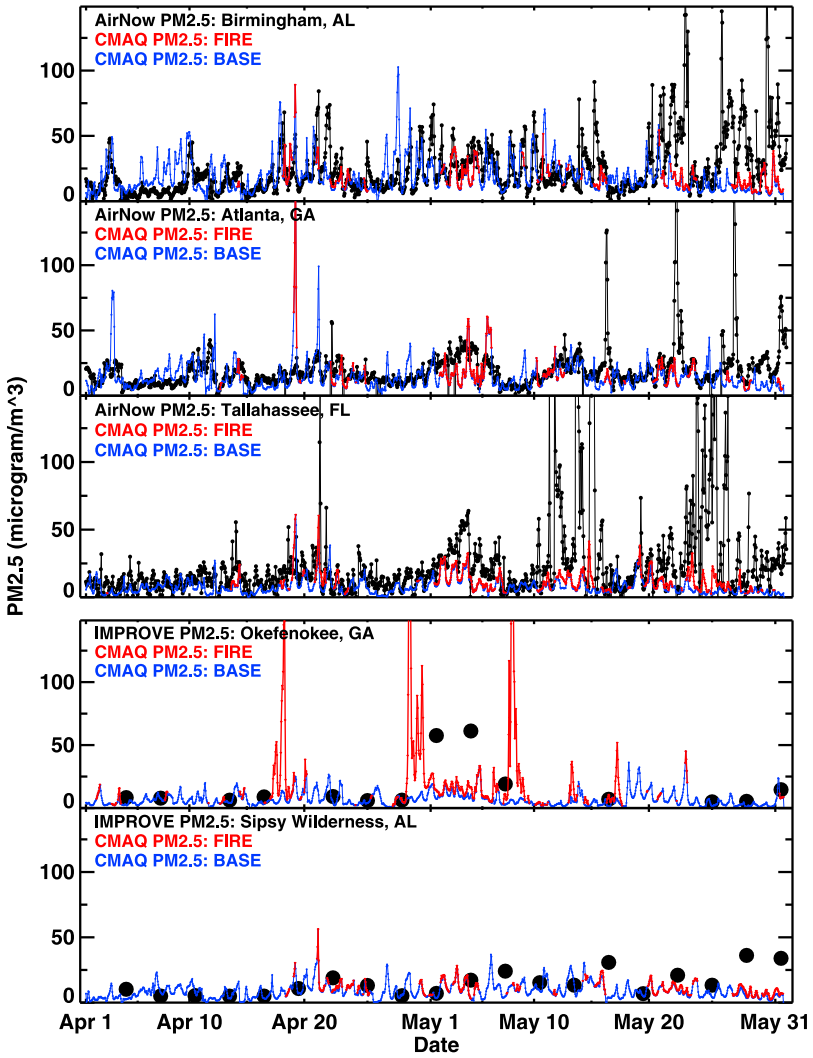

Figure 3. Surface-level hourly $PM_{2.5}$ concentrations in $\mu g\ m^{-3}$ at AirNow and IMPROVE stations for 1 April to 31 May 2007: AirNow TEOM and IMPROVE samplers (black), CMAQ BASE (blue), and CMAQ FIRE (red).

[23] A change in the vertical distribution of the fire emission injection did not help resolve this disagreement, whether the fire emissions are injected below the PBL height, equally below and above the PBL height, or into the lowest model layer. Our sensitivity studies indicated, relative to the CMAQ $PM_{2.5}$ simulations with fire emissions injected uniformly below the PBL height, (1) the surface-level $PM_{2.5}$ inside the plume increases by more than 50% at fire spots and gradually decreases up to about 30% when all fire emissions are injected into the lowest model layer and (2) the surface-level $PM_{2.5}$ inside the plume decreases by about 20–50% when the fire emissions are injected equally below and above the PBL height. Although the simulated $PM_{2.5}$ concentrations are significantly affected by the plume injection heights, the magnitude of changes is still much smaller than the difference between the simulated and observed $PM_{2.5}$. Importantly, the changes in plume injection height do not significantly affect the predicted position and shape of surface-level fire plumes. Therefore, the changes in plume injection height would not improve the comparison with the ground-based measurements of $PM_{2.5}$ unless the position of the fire plume is accurately simulated. *Stein et al.* [2009] also noted that in the case study of the 2007 Georgia and Florida fires, the change in plume injection height does not much improve their surface-level $PM_{2.5}$ simulations.

4.2. Top-Down Estimates of Fire Emissions of $PM_{2.5}$

[24] The GOES biomass burning emission algorithm is a tool of bottom-up estimates [*Zhang et al.*, 2008]. The bottom-up estimate of $PM_{2.5}$ tends to be underestimated due to uncertainties in input parameters for the emissions algorithm [*Wang et al.*, 2006; *Christopher et al.*, 2009; *Reid et al.*, 2009]. In order to directly compare with the MODIS AOT, the model-simulated aerosol species (mostly $PM_{2.5}$) mass concentrations are converted to AOT values using the empirical relationship between aerosol species mass concentrations and AOT, with the relative humidity correction

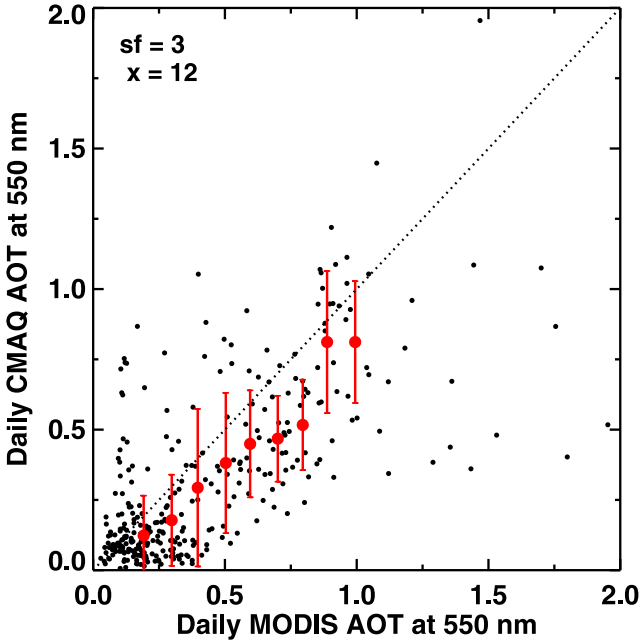

Figure 4. Scatterplot of daily MODIS AOT versus daily CMAQ AOT when the fire emissions of $PM_{2.5}$ are increased by a factor of 3 into CMAQ. The red dot with red vertical bar represents the average value within an AOT interval of 0.1 and its 1-sigma error range. The black dotted line shows the one-to-one correspondence line with a slope of 1.

due to particle size growth [e.g., *Binkowski and Roselle*, 2003]. The CMAQ-simulated AOT (CAOT) and observed MODIS AOT (MAOT) should have one-to-one correspondence with a slope of 1 if fire emissions of $PM_{2.5}$ are accurate and if transport and dispersion of fire plumes are well accounted for in CMAQ simulations. If fire emission inputs of $PM_{2.5}$ into CMAQ are underestimated, CAOT (predicted) will be systematically lower than MAOT (observed) near fire sources and downwind of fires, or vice versa. If transport and dispersion of fire plumes are not well represented in CMAQ, the predicted fire plumes at a certain location and time may not be seen from MODIS (false positive: predicted but not observed). In some other cases, the unpredicted smoke may be detected by MODIS (false negative: not predicted but observed).

[25] In order to compare the magnitude of CAOT with MAOT, we exclude the false positive and false negative situations that deteriorate the relationship between CAOT and MAOT during fires. However, the exclusion of the false positives and negatives may not be clear-cut because the plume density is significantly different between plume core and boundary. $PM_{2.5}$ concentrations could be predicted high but observed low, or predicted low but observed high even if the plume is both predicted and observed. These predicted $PM_{2.5}$ excess or deficit will also affect the relationship between CAOT and MAOT depending on the amount of excess or deficit $PM_{2.5}$. Therefore, we select the MODIS-CMAQ data pairs where dense fire plumes were present both in MODIS observations and CMAQ simulations with high probability. The MAOT and CAOT pair is selected if both magnitudes are x times larger than the CMAQ BASE AOT value. If x is small, there is more chance to have false positives and negatives. If x is large, there is more chance of selecting the MODIS-CMAQ data pairs inside dense fire plume. However, x should not be too large because only few data pairs would satisfy the condition. The CAOT magnitude can be expressed by

$$\mathrm{CAOT} = \mathrm{CMAQ\ BASE\ AOT} + sf \times (\mathrm{CMAQ\ FIRE\ AOT} - \mathrm{CMAQ\ BASE\ AOT}),$$

where sf is a scaling factor to be multiplied to ensure not to underestimate or overestimate the CAOT. Note that $sf = 1$ if CMAQ AOT is not underestimated or overestimated. A change in sf changes the slope of MAOT versus CAOT. With several iterations, we obtained nearly one-to-one correspondence with a slope of 1 when $x = 12$ and $sf = 3$ (see Figure 4). The scaling factor of 3 for $PM_{2.5}$ was also noticed by *Reid et al.* [2009] in the regions of CONUS Eastern for 2006–2008. Although their top-down approach is not the same as ours, but it may indicate a range of the scaling factor in the fire emission estimates.

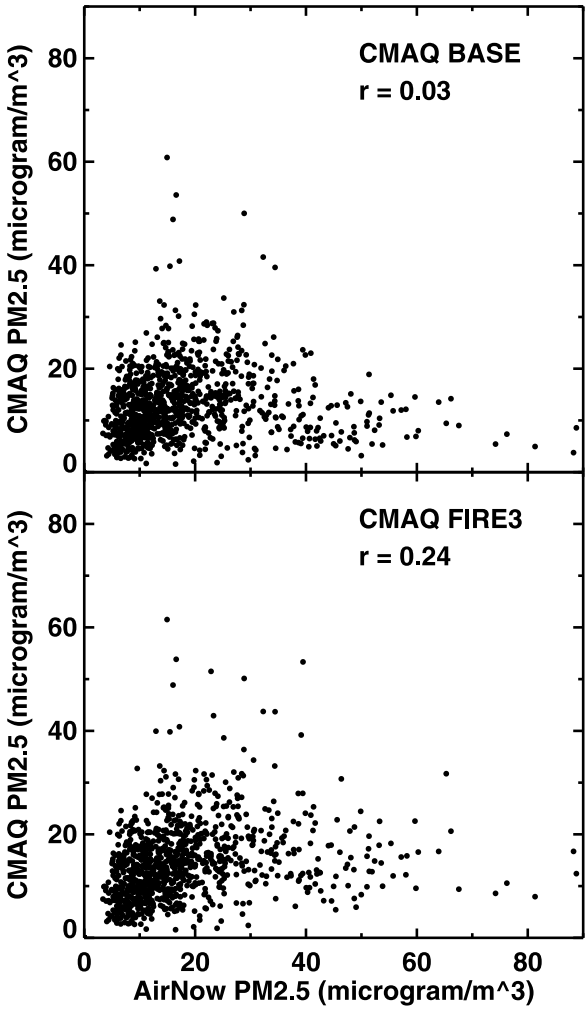

Figure 5. Scatterplot of daily AirNow $PM_{2.5}$ concentrations versus daily CMAQ $PM_{2.5}$ simulations (top) with baseline emissions (CMAQ BASE) and (bottom) with baseline plus three times of fire emissions (CMAQ FIRE3).

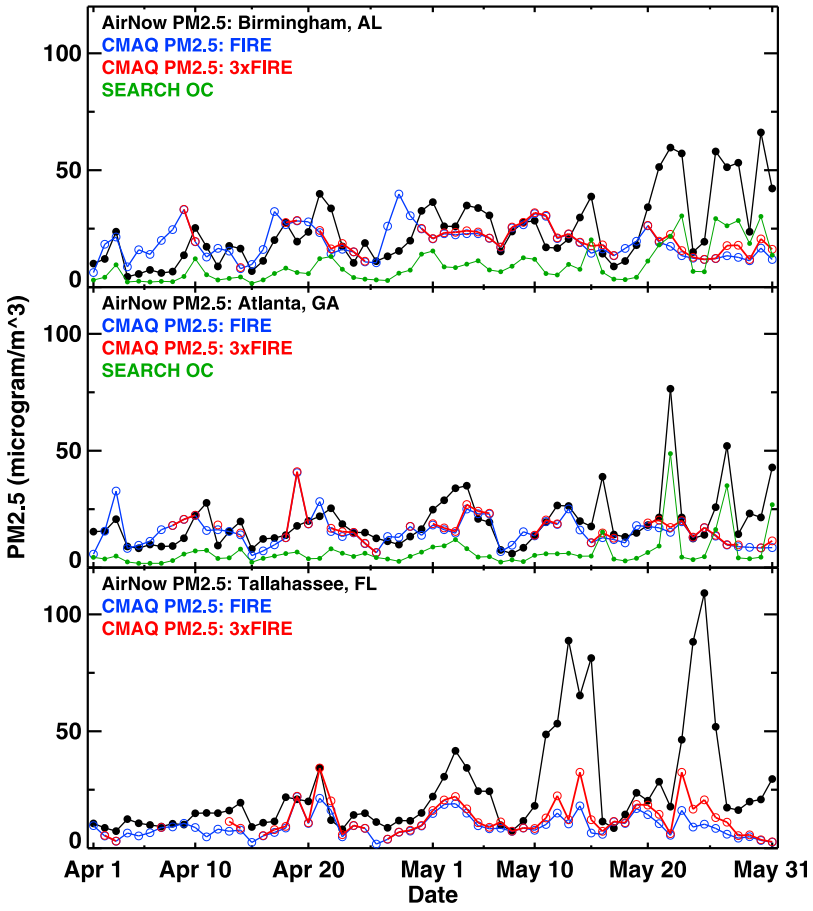

Figure 6. Comparison of daily AirNow $PM_{2.5}$ concentrations (black) at (top) Birmingham, (middle) Atlanta, and (bottom) Tallahassee with daily $PM_{2.5}$ concentrations for CMAQ FIRE (blue) and CMAQ FIRE3 (red). The daily SEARCH OC measurements are shown by the green line at Birmingham and Atlanta.

4.3. CMAQ Simulation of Fire Plumes With Uncertainty in Wind

[26] Tallahassee is of special interest because it is near the major fire source regions. The CMAQ FIRE run significantly underpredicts the observed $PM_{2.5}$ concentrations at Tallahassee in May 2007. For example, the averages of the CMAQ FIRE and observed $PM_{2.5}$ concentrations were 10.2 $\mu g\ m^{-3}$ and 65.7 $\mu g\ m^{-3}$ for 22–25 May 2007 (Figure 3). In order to reconcile the model with observations, the CMAQ is simulated with three times of the current fire emission rates (hereinafter referred to as FIRE3). Note that the scaling factor of three was introduced by the top-down approach described in section 4.2. The results are shown with the daily $PM_{2.5}$ observations at 17 AirNow stations in Alabama, Georgia, and northern Florida (Figure 5). The CMAQ FIRE3 improves the model performance for surface-level $PM_{2.5}$. The correlation coefficient was 0.04 for CMAQ BASE, increased to 0.12 for CMAQ FIRE (not shown), and became 0.24 for CMAQ FIRE3. CMAQ FIRE3, however, does not well simulate the outliers in the bottom right of the Figure 5 plots.

[27] The contribution of increased fire emissions of $PM_{2.5}$ is shown as the red line in Figure 6. Also shown in green are the daily organic carbon (OC) mass concentrations at the Southeastern Aerosol Research and Characterization Study (SEARCH) sites [*Hansen et al.*, 2003]. The high OC concentrations, mostly due to smoke aerosols originating from biomass burning, well indicate the sporadic fire smoke intrusions at Birmingham and Atlanta, especially in late May. Figure 6 shows that CMAQ FIRE3 improves the difference between the simulated and measured $PM_{2.5}$ concentrations, but the increase of $PM_{2.5}$ at Tallahassee was only 8.2 $\mu g\ m^{-3}$ for 22–25 May, far less than the amount that the model should have produced to be comparable to the observations. Since Tallahassee is at the boundary of fire plume in Figure 2, a small error in wind speed and direction might cause significant changes in $PM_{2.5}$ concentrations.

[28] Errors in wind speed and wind direction propagate into travel distance and direction of fire plumes, which increase uncertainty in predicted paths of fire plumes from fire spots. The u and v components of the Automated Surface Observing System (ASOS, details at http://www.nws.noaa.gov/asos) wind data (2-minutely in black) are shown with the surface wind in CMAQ (hourly in red) for April-May 2007 at Tallahassee (Figure 7). At first glance, these two data sets seem to agree well with each other. In fact, the mean difference between the hourly ASOS and hourly MM5 winds for April and May are 0.0 $m\ s^{-1}$ for u component and

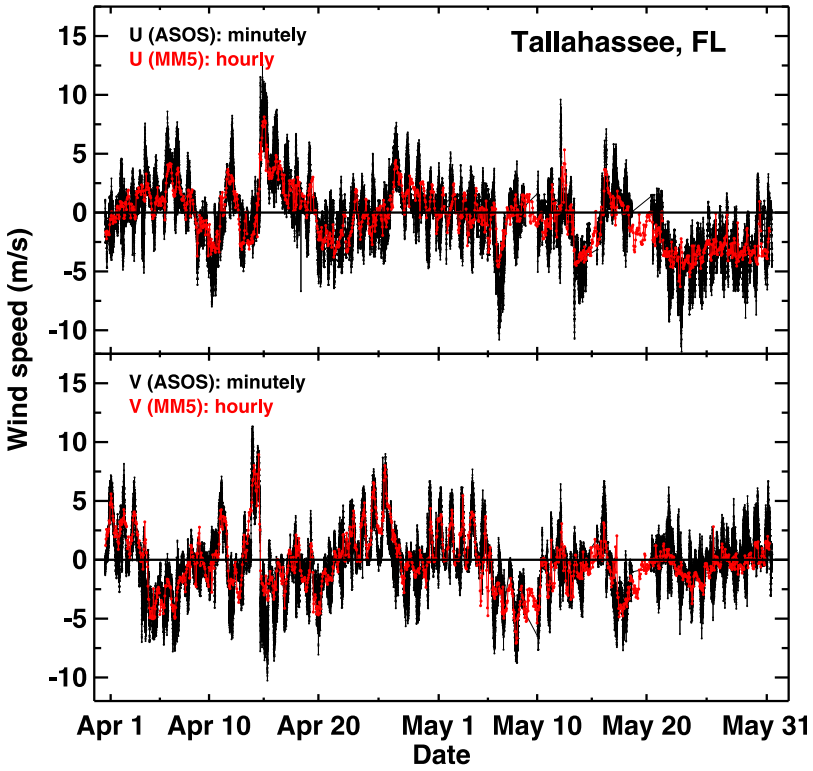

Figure 7. The (top) u and (bottom) v components of the ASOS and MM5 wind data for April–May 2007 at Tallahassee, Florida. The ASOS winds (black) are obtained every 2 min, and the MM5 winds (red) are hourly averages. Each tick in the *x* axis (date) represents local noon for each day.

0.1 m s^{-1} for v component of winds. This appears to have no significant bias between two data sets.

[29] Since the fire plume transport occurs within hours or days, we are more concerned about difference of the MM5 winds from the actual winds for a shorter time interval (hours or days). The ASOS winds are assumed as the actual winds in this study because the true winds cannot be obtained. Figure 8 shows a detailed comparison of the ASOS and MM5 winds at Tallahassee for 21–30 May 2007. The difference between the ASOS and MM5 winds is now clear for the data sets during hours or even during days. For example, on 23 May, the u component of the MM5 wind (red line) is overestimated and the v component is underestimated compared to those in the hourly ASOS (blue line), which could place the fire plume at Tallahassee toward southeast of the actual location.

[30] Although a transport pathway of a fire plume can be easily traced with forward trajectories using the MM5 winds, its systematic deviation from the actual position is not easily evaluated unless the MM5 wind bias is known. For comparison with the MM5 winds, the Rapid Update Cycle (RUC) analysis winds are assumed as close to the true winds. The RUC data used here have a horizontal resolution of 20 km with 37 vertical computational levels. In order to capture the transport pathway of $PM_{2.5}$ from fires, we use three-dimensional forward trajectories by using the following equation:

$$\mathbf{X}_{t+\Delta t}(x, y, p) = \mathbf{X}_t(x, y, p) + \mathbf{V}(\mathbf{X}_t(x, y, p))\Delta t,$$

where $\mathbf{X}_t$ and $\mathbf{V}_t$ give the position and velocity fields of a particle at longitude (x), latitude (y), pressure (p), and time (t). The time step (Δt) used is 5 min. The forward trajectories are computed using the MM5 and RUC analysis winds. We select the starting pressure level of low to middle PBL (e.g., 925 hPa) to better represent the PBL simulations of transport [*Stohl*, 1998].

[31] Although Figures 7 and 8 show the ASOS wind observations at 10 m and MM5 wind simulations at the lowest model layer (approximately at 10 m above the ground), the surface wind is not the major factor that drives transport of $PM_{2.5}$. It is rather the wind flow corresponding to the low to middle PBL [*Stohl*, 1998, and references therein]. Figure 9 shows an example of 24 h forward trajectories of a fire plume starting from the major fire spot (82.36°W and 30.81°N), pressure level at 925 hPa, and time on 0000 UT, 26 May 2007. At 18Z, the trajectory using the RUC analysis winds (red line) reaches closely to Birmingham. At the same time, the trajectory using the MM5 winds (blue line) is more than 200 km away from Birmingham. Although the trajectory does not show the actual size and shape of the fire plume, the distance is too far to affect the $PM_{2.5}$ concentrations at Birmingham. Indeed the daily $PM_{2.5}$ concentration of about 60 μg m^{-3} at Birmingham, as seen in Figure 6, was not simulated by CMAQ FIRE3 on 26 May. Since the MM5 winds placed the fire plume far away from Birmingham, the increase of fire emissions by three times little affected the CMAQ $PM_{2.5}$ at Birmingham. The RUC winds appear to be accurate on 26 May, but note that they are not the true winds either and are also subject to

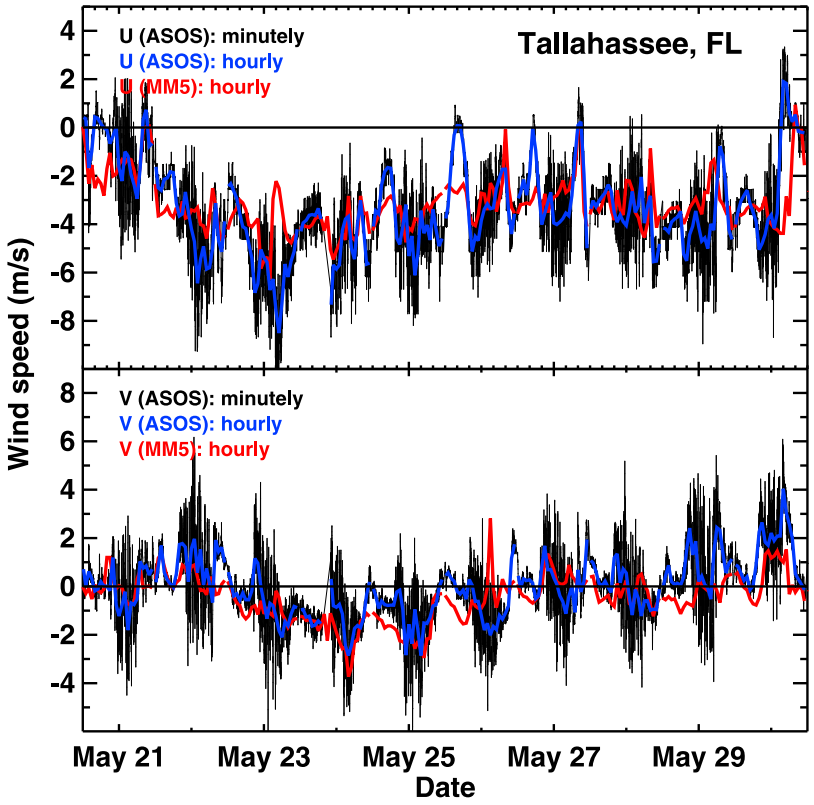

Figure 8. Same as Figure 7 but with the detailed view of (top) u and (bottom) v components of the ASOS and MM5 wind data for 21–30 May 2007 at Tallahassee, Florida. The hourly mean of ASOS winds are shown in blue for comparison with the hourly MM5 winds (red). Each tick in the *x* axis (date) represents local noon for each day.

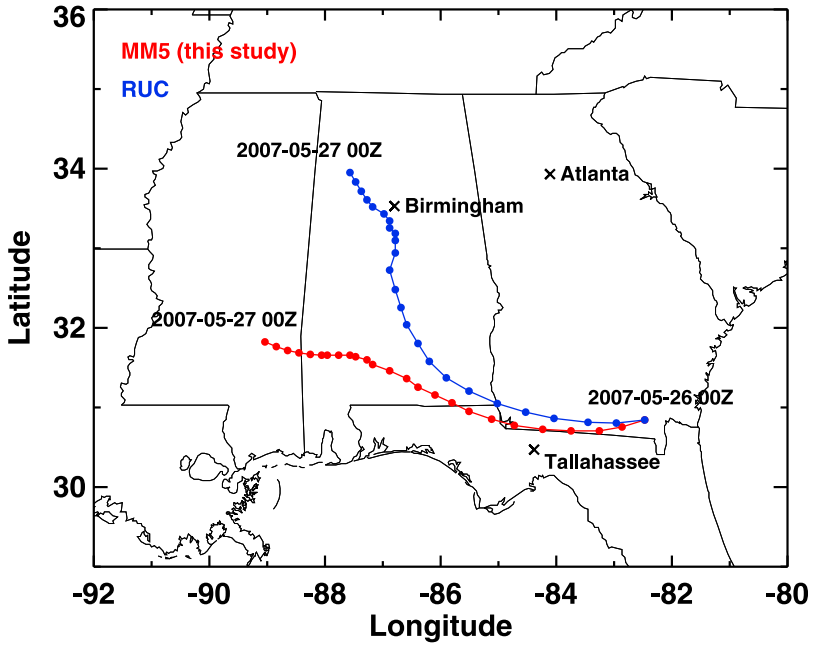

Figure 9. Twenty-four hour forward trajectories, starting at 0000 UT on 26 May from a major fire source in Georgia at 925 hPa. The trajectories are calculated using the MM5 (red line) and RUC analysis wind fields (blue line). The AirNow stations are shown as crosses at Tallahassee, Birmingham, and Atlanta.

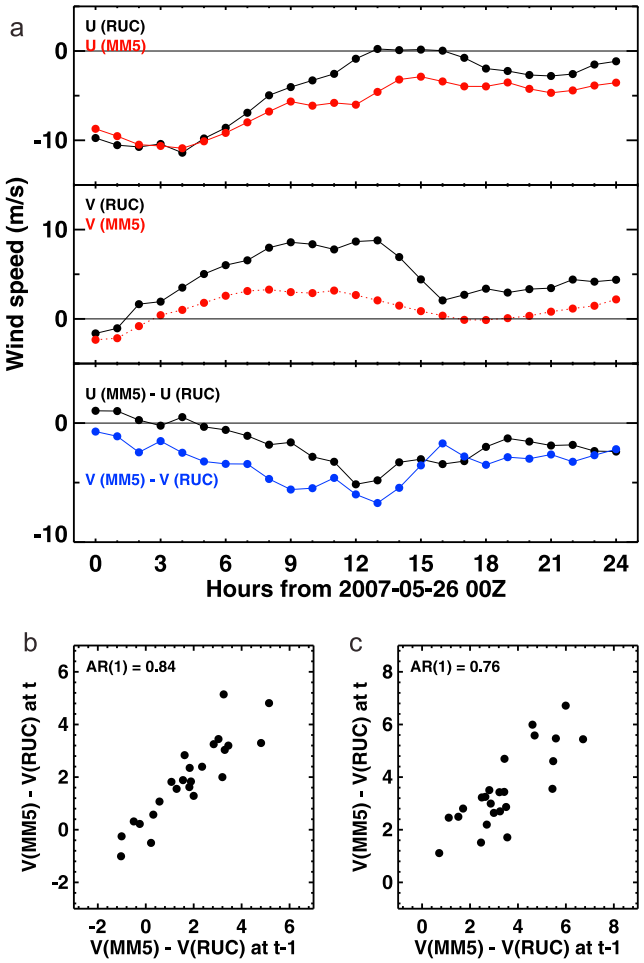

Figure 10. (a) The u and v components of RUC (black) and MM5 (red) winds following the trajectories in Figure 9. The difference in u and v components of winds between two data sets is shown in Figure 10a (bottom). To show autocorrelation, the wind difference at time t-1 is compared with that at time t for (b) u component and (c) v component.

bias. This example shows that transport error could dominate the accuracy of CMAQ FIRE irrespective of the assumption concerning plume injection height and uncertainty in fire emission estimates.

[32] The overall root mean square error of u and v components of the MM5 wind is less than 2 m s^{-1} at the four ASOS stations: Birmingham, Atlanta, Tallahassee, and Jacksonville in Florida. These wind error estimates well agree with the previous intensive estimates of the MM5 wind errors in the southeastern United States [e.g., *Emery et al.*, 2001; *Olerud and Sims*, 2004], which showed the wind speed error less than 2 m s^{-1} and wind direction error of less than 30 degrees. The standard error of the MM5 winds are also estimated as 2–3 m s^{-1} by comparing the MM5 winds with the RUC analysis winds at each hourly segment of the 24 h forward trajectories starting from the major fire spots at 925 hPa for April–May. Figure 10a shows a comparison of the MM5 with the RUC analysis winds at each hourly segment of trajectories shown in Figure 9. If the difference between the MM5 and ASOS (or RUC) winds were serially random, the position error at Birmingham would have been increased with the square root of the number of time step. However, the MM5 wind errors in Figures 8 and 10 are not independent of each other, but highly skewed toward positive or negative at least at the short time scales (a day or less). This positive serial correlation of wind errors introduces undesirable systematic deviations of predicted fire plumes from the actual locations.

[33] Time series of difference between the MM5 wind and RUC analysis winds (and ASOS surface winds) show a positive autocorrelation (Figures 10b and 10c). The first-order autoregressive, AR(1), coefficient ranges from 0.75 to 0.95 for the model period. If the model simulated wind error were independent of each other, the present wind error would not have been affected by the past wind error. In this case, the present wind error could have been positive or negative with equal probability. However, if there is a positive autocorrelation between the past and present wind errors, the present wind error should be affected by the past error. For example, if the past wind error happened to be positive, the present wind error is more likely to be positive. If the errors tend to be positive, the deviation of fire plume from its actual location increases over time, more quickly than that of the case when the error was not serially correlated. The transport perspective of this deviation is critical to accurately locate fire plumes if fire plume transport occurs within days or shorter (local and regional scales). However, a thorough treatment of this topic is beyond the scope of this study. The position error estimates with AR(1) term will be discussed in the next study.

5. Summary

[34] The impact of fire emissions on surface-level $PM_{2.5}$ are investigated during the Georgia and Florida fires in 2007. The satellite-derived fire times, locations, and emission rates are used as inputs to the CMAQ chemical transport model. The CMAQ simulations reproduce the overall transport features of satellite-retrieved AOT and TCO. The surface-level $PM_{2.5}$ concentrations downwind of fires are significantly elevated in the CMAQ simulations by adding fire emissions. However, the simulations are not satisfactory in that the sporadic fire episodes detected from the ground-based $PM_{2.5}$ measurements are not well reproduced in the CMAQ $PM_{2.5}$ in terms of magnitude and location. A comparison of CMAQ-derived AOT with MODIS AOT suggests the $PM_{2.5}$ fire emissions should be increased by a factor of 3. The increase in the fire emission rates partly reconciles the difference between the CMAQ predictions and ground-based $PM_{2.5}$ observations, but the predicted $PM_{2.5}$ concentrations are still far less than the ground-based observations.

[35] We examine the role of uncertainty in smoke transport at Tallahassee, Birmingham, and Atlanta. The long-term averages of the model simulated winds for April and May do not show a significant bias compared to the ground-based surface wind observations (and RUC analysis winds). The difference, however, becomes particularly noticeable and even systematic when two wind data sets are compared for short time intervals, days or hours. The drift behavior of the model simulated wind errors is explained by the first-order autoregressive processes that make the transport error

grow rapidly with each time step. Since the smoke transport in this study mostly occurs within hours and days (local and regional scales), the short-term error in the model simulated winds is critical to accurately locate the fire plumes. Therefore failure of predicting the high $PM_{2.5}$ concentrations at Birmingham, Atlanta, and Tallahassee is most likely due to uncertainty in transport models. A further modeling study, which accounts for wind errors with AR(1), is needed to better estimate the position error of predicted fire plumes.

[36] **Acknowledgments.** This research was sponsored by NOAA Air Quality projects at University of Alabama in Huntsville. MODIS data were obtained from Atmosphere Archive and Distribution System (LAADS) at Goddard Space Flight Center (GSFC). $PM_{2.5}$ data were obtained from EPA's Air Quality System (AQS).

References

Al-Saadi, J., et al. (2005), Improving national air quality forecasts with satellite aerosol observations, *Bull. Am. Meteorol. Soc.*, *86*(9), 1249–1261, doi:10.1175/BAMS-86-9-1249.

Barnard, W. R., and E. Sabo (2008), Documentation of the Base G2 and Best & Final 2002 Base Year, 2009 and 2018 Emission Inventories for VISTAS, report, VISTAS, Forest Park, Calif.

Bey, I., D. J. Jacob, R. M. Yantosca, J. A. Logan, B. D. Field, A. M. Fiore, Q. Li, H. Y. Liu, L. J. Mickley, and M. G. Schultz (2001), Global modeling of tropospheric chemistry with assimilated meteorology: Model description and evaluation, *J. Geophys. Res.*, *106*(D19), 23,073–23,095, doi:10.1029/2001JD000807.

Binkowski, F. S., and S. J. Roselle (2003), Models-3 Community Multiscale Air Quality (CMAQ) model aerosol component: 1. Model description, *J. Geophys. Res.*, *108*(D6), 4183, doi:10.1029/2001JD001409.

Byun, D., and K. L. Schere (2006), Review of the governing equations, computational algorithms, and other components of the Models-3 Community Multiscale Air Quality (CMAQ) modeling system, *Appl. Mech. Rev.*, *59*, 51–77, doi:10.1115/1.2128636.

Christopher, S. A., P. Gupta, U. Nair, T. A. Jones, S. Kondragunta, Y. Wu, J. Hand, and X. Zhang (2009), Satellite remote sensing and mesoscale modeling of the 2007 Florida/Georgia fires, *IEEE J. Sel. Topics Appl. Earth Obs. Remote Sens.*, *26*, 1–13.

Colarco, P. R., M. R. Schoeberl, B. G. Doddridge, L. T. Marufu, O. Torres, and E. J. Welton (2004), Transport of smoke from Canadian forest fires to the surface near Washington, D.C.: Injection height, entrainment, and optical properties, *J. Geophys. Res.*, *109*, D06203, doi:10.1029/2003JD004248.

Draxler, R. R., and G. D. Hess (1997), Description of the HYSPLIT_4 modeling system, rev. January 2004, *NOAA Tech. Memo. ERL ARL-224*, NOAA, Washington, D. C.

Edgerton, E. S., B. E. Hartsell, R. D. Saylor, J. J. Jansen, D. A. Hansen, and G. M. Hidy (2005), The Southeastern Aerosol Research and Characterization Study: Part II. Filter-based measurements of fine and coarse particulate matter mass and composition, *J. Air Waste Manage. Assoc.*, *55*, 1527–1542.

Emery, C., E. Tai, and G. Yarwood (2001), Enhanced Meteorological Modeling and Performance Evaluation for Two Texas Episodes, Int. Corp., Novato, Calif.

Engel-Cox, J. A., H. H. Christopher, B. W. Coutant, and R. M. Hoff (2004), Qualitative and quantitative evaluation of MODIS satellite sensor data for regional and urban scale air quality, *Atmos. Environ.*, *38*, 2495–2509, doi:10.1016/j.atmosenv.2004.01.039.

Gery, M. W., G. Z. Whitten, J. P. Killus, and M. C. Dodge (1989), A photochemical kinetics mechanism for urban and regional scale computer modeling, *J. Geophys. Res.*, *94*(D10), 12,925–12,956, doi:10.1029/JD094iD10p12925.

Grell, G. A., J. Dudhia, and D. R. Stauffer (1995), A description of the Fifth-Generation Penn State/NCAR Mesoscale Model (MM5), *NCAR Tech. Note NCAR/TN 398+STR*, 138 pp., NCAR, Boulder, Colo.

Grover, B. D., M. Kleinman, N. L. Eatough, D. J. Eatough, P. K. Hopke, R. W. Long, W. E. Wilson, M. B. Meyer, and J. L. Ambs (2005), Measurement of total $PM_{2.5}$ mass (nonvolatile plus semivolatile) with the filter dynamic measurement system tapered element oscillating microbalance monitor, *J. Geophys. Res.*, *110*, D07S03, doi:10.1029/2004JD004995.

Gupta, P., and S. A. Christopher (2008), Seven year particulate matter air quality assessment from surface and satellite measurements, *Atmos. Chem. Phys.*, *8*, 3311–3324, doi:10.5194/acp-8-3311-2008.

Hansen, D. A., E. S. Edgerton, B. E. Hartsell, J. J. Jansen, N. Kandasamy, G. M. Hidy, and C. L. Blanchard (2003), The Southeastern Aerosol Research and Characterization Study: Part 1—Overview, *J. Air Waste Manage. Assoc.*, *53*, 1460–1471.

Hertel, O., R. Berkowicz, J. Christensen, and O. Hov (1993), Test of two numerical schemes for use in atmospheric transport-chemistry models, *Atmos. Environ., Part A*, *27*, 2591–2611.

Houyoux, M. R., J. M. Vukovich, C. J. Coats Jr., N. J. M. Wheeler, and P. Kasibhatla (2000), Emission inventory development and processing for the seasonal model for regional air quality (SMRAQ) project, *J. Geophys. Res.*, *105*(D7), 9079–9090, doi:10.1029/1999JD900975.

Larkin, N. K., S. M. O'Neill, R. Soloman, C. Krull, S. Raffuse, M. Rorig, J. Peterson, and S. Ferguson (2009), The BlueSky smoke modeling framework: Design, application, and performance, *Int. J. Wildland Fire*, *18*, 906–920, doi:10.1071/WF07086.

Malm, W. C., B. A. Schichtel, M. L. Pitchford, L. L. Ashbaugh, and R. A. Eldred (2004), Spatial and monthly trends in speciated fine particle concentration in the United States, *J. Geophys. Res.*, *109*, D03306, doi:10.1029/2003JD003739.

Marmur, A., S.-K. Park, J. A. Mulholland, P. E. Tolbertb, and A. G. Russell (2006), Source apportionment of $PM_{2.5}$ in the southeastern United States using receptor and emissions-based models: Conceptual differences and implications for time-series health studies, *Atmos. Environ.*, *40*, 2533–2551, doi:10.1016/j.atmosenv.2005.12.019.

Mathur, R. (2008), Estimating the impact of the 2004 Alaskan forest fires on episodic particulate matter pollution over the eastern United States through assimilation of satellite-derived aerosol optical depths in a regional air quality model, *J. Geophys. Res.*, *113*, D17302, doi:10.1029/2007JD009767.

McMillan, W. W., et al. (2008), AIRS views transport from 12 to 22 July 2004 Alaskan/Canadian fires: Correlation of AIRS CO and MODIS AOD with forward trajectories and comparison of AIRS CO retrievals with DC-8 in situ measurements during INTEX-A/ICARTT, *J. Geophys. Res.*, *113*, D20301, doi:10.1029/2007JD009711.

Olerud, D., and A. Sims (2004), MM5 2002 Modeling in Support of VISTAS (Visibility Improvement-State and Tribal Association of the Southeast), report, VISTAS, Forest Park, Calif.

Pierce, T., C. Geron, G. Pouliot, E. Kinnee, and J. Vukovich (2002), Integration of the Biogenic Emission Inventory System (BEIS3) into the Community Multiscale Air Quality Modeling System, paper presented at 12th Joint Conference on the Applications of Air Pollution Meteorology with the Air and Waste Management Association, Am. Meteorol. Soc., Norfolk, Va.

Reid, J. S., et al. (2009), Global monitoring and forecasting of biomass-burning smoke: Description of and lessons from the Fire Locating and Modeling of Burning Emissions (FLAMBE) program, *IEEE J. Sel. Topics Appl. Earth Obs. Remote Sens.*, *2*, 144–162, doi:10.1109/JSTARS.2009.2027443.

Remer, L. A., et al. (2005), The MODIS aerosol algorithm, products and validation, *J. Atmos. Sci.*, *62*, 947–973, doi:10.1175/JAS3385.1.

Rolph, G. D., et al. (2009), Description and verification of the NOAA Smoke Forecasting System: The 2007 fire season, *Weather Forecast.*, *24*, 361–378, doi:10.1175/2008WAF2222165.1.

Roy, B., G. A. Pouliot, A. Gilliland, T. Pierce, S. Howard, P. V. Bhave, and W. Benjey (2007), Refining fire emissions for air quality modeling with remotely sensed fire counts: A wildfire case study, *Atmos. Environ.*, *41*, 655–665, doi:10.1016/j.atmosenv.2006.08.037.

Ruminski, M., and S. Kondragunta (2006), Monitoring fire and smoke emissions with the hazard mapping system, *SPIE Int. Soc. Opt. Eng.*, *6412*, 64120B, doi:10.1117/12.694183.

Seiler, W., and P. J. Crutzen (1980), Estimates of gross and net fluxes of carbon between the biosphere and the atmosphere from biomass burning, *Clim. Change*, *2*, 207–247, doi:10.1007/BF00137988.

Stein, A. F., G. D. Rolph, R. R. Draxler, B. Stunder, and M. G. Ruminski (2009), Verification of the NOAA Smoke Forecasting System: Model sensitivity to the injection height, *Weather Forecast.*, *24*, 379–394, doi:10.1175/2008WAF2222166.1.

Stohl, A. (1998), Computation, accuracy and applications of trajectories—A review and bibliography, *Atmos. Environ.*, *32*, 947–966, doi:10.1016/S1352-2310(97)00457-3.

Susskind, J., C. D. Barnet, and J. M. Blaisdell (2003), Retrieval of atmospheric and surface parameters from AIRS/AMSU/HSB data in the presence of clouds, *IEEE Trans. Geosci. Remote Sens.*, *41*, 390–409, doi:10.1109/TGRS.2002.808236.

Wang, J., S. A. Christopher, U. S. Nair, J. S. Reid, E. M. Prins, J. Szykman, and J. L. Hand (2006), Mesoscale modeling of Central American smoke transport to the United States: 1. "Top-down" assessment of emission strength and diurnal variation impacts, *J. Geophys. Res.*, *111*, D05S17, doi:10.1029/2005JD006416.

Zhang, X., and S. Kondragunta (2008), Temporal and spatial variability in biomass burned areas across the USA derived from the GOES fire product, *Remote Sens. Environ.*, *112*, 2886–2897, doi:10.1016/j.rse.2008.02.006.

Zhang, X., S. Kondragunta, C. Schmidt, and F. Kogan (2008), Near real time monitoring of biomass burning particulate emissions ($PM_{2.5}$) across contiguous United States using multiple satellite instruments, *Atmos. Environ.*, *42*, 6959–6972, doi:10.1016/j.atmosenv.2008.04.060.

Zhang, Y., K. Vijayaraghavan, X.-Y. Wen, H. E. Snell, and M. Z. Jacobson (2009), Probing into regional ozone and particulate matter pollution in the United States: 1. A 1 year CMAQ simulation and evaluation using surface and satellite data, *J. Geophys. Res.*, *114*, D22304, doi:10.1029/2009JD011898.

S. A. Christopher and E.-S. Yang, Earth System Science Center, University of Alabama in Huntsville, 320 Sparkman Dr., Huntsville, AL 35806-1912, USA. (yes@nsstc.uah.edu)

S. Kondragunta and X. Zhang, Center for Satellite Applications and Research, NESDIS, NOAA, Camp Springs, MD 20746, USA.